REPORT DOCUMENTATION PAGE

Form Approved
OMB No. 0704-0188

1. REPORT DATE *(DD-MM-YYYY)*

2. REPORT TYPE
Technical Papers

3. DATES COVERED *(From - To)*

4. TITLE AND SUBTITLE

Please see attached

5a. CONTRACT NUMBER

5b. GRANT NUMBER

5c. PROGRAM ELEMENT NUMBER

6. AUTHOR(S)

5d. PROJECT NUMBER
2308

5e. TASK NUMBER
M13C

5f. WORK UNIT NUMBER
346057

7. PERFORMING ORGANIZATION NAME(S) AND ADDRESS(ES)

Air Force Research Laboratory (AFMC)
AFRL/PRS
5 Pollux Drive
Edwards AFB CA 93524-7048

8. PERFORMING ORGANIZATION REPORT

9. SPONSORING / MONITORING AGENCY NAME(S) AND ADDRESS(ES)

Air Force Research Laboratory (AFMC)
AFRL/PRS
5 Pollux Drive
Edwards AFB CA 93524-7048

10. SPONSOR/MONITOR'S ACRONYM(S)

11. SPONSOR/MONITOR'S NUMBER(S)
Please see attached

12. DISTRIBUTION / AVAILABILITY STATEMENT

Approved for public release; distribution unlimited.

13. SUPPLEMENTARY NOTES

14. ABSTRACT

20030121 094

15. SUBJECT TERMS

16. SECURITY CLASSIFICATION OF:			17. LIMITATION OF ABSTRACT	18. NUMBER OF PAGES	19a. NAME OF RESPONSIBLE PERSON
					Leilani Richardson
a. REPORT	b. ABSTRACT	c. THIS PAGE			19b. TELEPHONE NUMBER *(include area code)*
Unclassified	Unclassified	Unclassified	A		(661) 275-5015

Standard Form 298 (Rev. 8-98)
Prescribed by ANSI Std. 239.18

TP-FY99-ØØ89

d308MI 36

ERC # E99-004 (letter missing)

✓ Spreadsheet

✓ DTB

MEMORANDUM FOR PRR (~~Contractor~~ In-House Publication)

FROM: PROI (TI) (STINFO)

4 May 1999

SUBJECT: Authorization for Release of Technical Information, Control Number: AFRL-PR-ED-TP-FY99-0089 Chehroudi, Talley and Coy. "Anatomical Changes of a Cryogenic Jet in Transition to the Thermodynamic Supercritical Condition"

(Public Release)

ANATOMICAL CHANGES OF A CRYOGENIC JET IN TRANSITION TO THE THERMODYNAMIC SUPERCRITICAL CONDITION

B. Chehroudi[*], *D. Talley, and E. Coy*

Air Force Research Laboratory, AFRL/PRSA
10 E. Saturn Boulevard
Edwards AFB, CA 93524-7680

ABSTRACT

The high pressure supercritical facility at AFRL is used to investigate effects of chamber pressure (density) ranging from the thermodynamic subcritical to supercritical values at a supercritical chamber temperature. At subcritical pressures, the jets exhibit wave-like structures which amplify downstream and eventually break up into irregularly-shaped small entities. The formation of many droplets is seen at higher pressures, resembling a second wind-induced liquid-jet breakup. Further increase of chamber pressure, near the critical condition, fails to induce the transition into a full liquid atomization regime. At this point, the jet anatomy changes abruptly to imitate turbulent gas jet injection. The jet initial growth rate is plotted against the chamber-to-injectant density ratio, along with available data on other liquid/gaseous jets and mixing layers, producing a unique and informative graph. For supercritical conditions, our measured growth rate agrees well with a theoretical equation proposed by Papamoschou and Roshko [1] and closely follows the trend of Dimotakis [2] for incompressible but variable-density gaseous turbulent mixing layers. Fractal analysis of the jet interface also shows a similarity to gas jet behavior with comparable fractal dimension. This is the first time quantitative evidence has been provided to support qualitative visualizations suggesting that supercritical jets appear to behave like conventional gas jets.

INTRODUCTION

A general trend to operate under an increasingly higher combustor pressures is observed in rockets, gas turbines, and diesel engines, primarily due to enhanced effects on thrust, power, or efficiency. Under such conditions, the environment into which fuel is injected can be at a supercritical state. This motivated a systematic investigation at AFRL to initially document, analyze, and finally understand anatomical changes of a liquid cryogenic jet subjected to a transition from subcritical to supercritical conditions, as occurs in the thrust chamber environment of a cryogenic chemical rocket. As examples, the Space Shuttle main engine thrust chamber pressure is about 22.3 MPa. And, the combustion chamber pressure for Vulcain (Ariane 5) with liquid H_2 (P_c=1.27 MPa, T_c=33.25 K)/liquid O_2 (P_c= 5.043 Mpa, T_c=154.58 K) can reach up to 10 MPa while a record pressure of nearly 28.2 MPa has been reported. Very little information is available on liquid jets injected into supercritical environment.

For a pure substance, the distinction between liquid and gas phases disappears at and above the critical pressure (called as "fluid") and density, thermal conductivity, mass diffusivity, and surface tension show large variations near the critical point. At elevated ambient pressure, the solubility of gases into the liquid phase increases and multicomponent phase equilibrium information, or "critical mixing temperature or pressure," should be used, see *Bruno and Ely [3]*. Hence, when a pure liquid fuel drop is introduced into a gas, a thin layer that is a mixture of that gas and the fuel is formed on the surface that spreads spatially in time. In what follows, the terms subcritical and supercritical, and the reduced pressure (P_r) and temperature (T_r), are referenced with respect to the critical condition of the pure substance used in the drops or jets, and not the environment.

Recently, some results on liquid jet injection into supercritical condition have been presented, for example *Newman and Brzustowski [4]* and *Mayer et al.[5], [6], and Chen and Sui [7]* at high Reynolds numbers and *Woodward and Talley [8]* at low Reynolds numbers. *Newman and Brzustowski [9]* proposed the possibility of gasification and that at supercritical temperatures and pressures the jet can be considered as a variable-density single-phase turbulent submerged gas jet. Also, assuming self-preserving flow, negligible gravity, zero latent heat of vaporization, ideal gas

behavior, and thermal equilibrium between gas and drops, they developed a model for predicting the profile of the outer extent of a supercritical steady jet. Comparison with experiment was poor near the injector. *Mayer et al [6]* used a liquid N_2 (LN_2) jet at 105 K into a N_2 environment at 300 K but at varying ambient sub- to supercritical pressures and observe that the jet behaves similar to the classical atomization of liquid fuel with ligaments and drops below the critical pressure. They report gas-jet like appearance with no evidence of droplets at supercritical conditions. For an N_2-into-N_2 cryogenic jet, *Woodward and Talley [8]* showed that the addition of He gas to the supercritical ambient N_2 fluid forced the jet to look like injection into the subcritical ambient condition.

EXPERIMENTAL SETUP

The stainless steel chamber in Fig. 1 can withstand pressures and temperatures of up to 137 atm (2000 psi) and 473 K, respectively, and has two facing circular sapphire windows and two UV-grade side-mounted slot-shaped quartz windows for laser in/out of the chamber. Transport of the liquid through the lines and the injector is achieved as shown in Figure 1. The liquid N_2 from a dewar is used to cool and/or liquefy the injectant passing through the cryogenic cooler prior to injection. In addition to N_2, a branch is connected for possibly introducing other gases or mixtures of gases as a chamber medium. The mass flow rate of the injectant is regulated and also measured via a mass flowmeter, and a precision micrometer valve. For more details refer to *Woodward and Talley [8] and Chehroudi et al. [9]*. The injection in this study is through a sharp-edged 50-mm long stainless steel tube with 1.59-mm (1/16")-in. diameter and a 254-micron (0.010")-in. inner hole (length-to-diameter ratio of 200). With the Reynolds number ranging from 25,000 to 70,000, the entrance length from 50 to 100 is needed, see *Schlichting [10]*. The length is therefore long enough to ensure fully-developed turbulent pipe flow at the exit. The rig is fully instrumented with thermocouples, pressure gages and transducers, and mass flowmeters at the locations indicated in Fig. 1. Back-illumination and a model K2 Infinity long-distance microscope is used with a TM-745E high resolution (768(H) x 493(V) pixels in 8.8(H)x6.6(V) mm actual sensing area) interlaced CCD camera by PULNix to form images of the injected jets. For more details refer to *Chehroudi et al. [9]*.

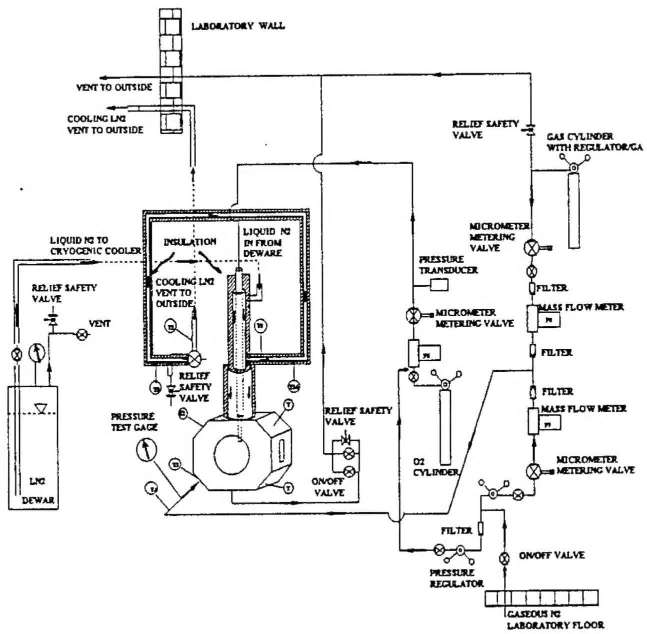

Figure 1. Schematic diagram of experimental setup for sub- to supercritical jet injection

ANATOMICAL CHANGES OF THE JET

Figure 3 shows images of the N_2 jet injected into N_2 at a fixed supercritical chamber temperature but varying sub- to supercritical pressure. At the lowest subcritical chamber pressure, the jet is liquid-like with surface instabilities that grow downstream. Very fine drops are seen ejecting from the jet at P_r of 0.83 and the jet grows away from the injector. There are major structural/interface changes at P_r of 1.03 and no drops are detected with the highest magnification used to view these high resolution images. Thread- or finger-like entities seen at the interface are not broken up into droplets and are seemingly dissolved at different distances from the jet dark-core region. This forms a mixing layer in which phase transition and/or large local density non-uniformities occur. A further increase of chamber pressure decreases the length and the thickness of the internal dark core, and images progressively resemble injection of a gaseous turbulent jet into a gaseous environment (see magnified images in Fig. 4). A gradual transition from a classical liquid-like appearance in which ligaments and drops are formed at the interface in the liquid atomization regime to a comb-like structure near the critical point, and finally to where a submerged turbulent gas jet appearance emerges can be observed. Inspecting a large set of images at high magnifications, no evidence of drop formation is seen in this gas-like jet regime. The reason for this behavior, particularly for the change into gas-jet like behavior, should be sought in progressive reduction of surface tension and heat of vaporization until they both vanish at and above the critical point. Similar observations are made for the O_2-into-N_2 case but with the transition to gas-like jet at near the oxygen critical pressure (P_r = 0.85). Observation of the gas-like jet behavior and the lack of any drop formation raises a question on the relevancy of current injection models and some drop vaporization/combustion results within this regime.

Traditionally, the breakup and atomization regimes of the liquid jet within a narrow chamber-to-density ratio range is shown on a plot of Ohnesorge number versus Reynolds number (ignoring gas density and nozzle geometrical factors) or by a more refined criterion of *Reitz and Bracco [11]* in which chamber-to-injectant density ratio, nozzle geometrical factor, and Weber and Reynolds numbers are all included. In Fig. 3, as chamber pressure approaches the critical condition, surface tension is reduced to a near-zero value and for the range of Reynolds number calculated here (25,000 to 75,000), the Ohnesorge number sharply swings from a low (estimated to be 2.8×10^{-3}) to a very large (infinity when surface tension is zero) values. The large Ohnesorge number regime and its importance are indicated in *Faeth [12]* and *Tseng et al. [13]*. At the low Ohnesorge number in this work, the second-wind induced liquid jet breakup behavior is observed, see Fig. 3. Past the second wind-induced behavior, it seems that before the jet has the opportunity for full atomization, the surface tension is sufficiently and rapidly reduced so one achieves gas-like jet appearance near but before reaching the critical pressure value, see Fig. 3. The aforementioned threads or fingers are gasified and no drops are detected. Transition into a full atomization regime is therefore inhibited. The investigated jet exhibits liquid-jet like and gas-jet like features depending on the magnitudes of the surface tension and heat of vaporization. Approximate characteristic time estimates by *Chehroudi et al. [9]* also point towards inhibition of the atomization.

JET GROWTH RATE

The initial jet spreading angle or its growth rate is measured for all acquired images and results along with those of others are presented in Fig. 5. The angles in our work are measured from the information within a 7-mm distance close to the injector exit face (distance-to-diameter ratio of up to 28). *Chehroudi et al [9]* show that the intact core of the liquid sprays, *Chehroudi et al [15],* and the potential core for different jets, *Abramovich [14],* have comparable lengths to the streamwise extent of the initial region used for the growth rate measurements, therefore ensuring the existence of the mixing layer. The importance and justification of the data sets selected in Fig. 5 and the nature of their measurements by other researchers are elaborated with sufficient details in our earlier paper to provide a deeper appreciation of ~~the~~ Fig. 5 and its uniqueness, see *Chehroudi et al. [9]*. Since the jets investigated here exhibit both liquid-like and gas-like jet appearances, appropriate results for both are presented in Fig. 5. The simplest is the prediction of the linear jet growth for the turbulent incompressible submerged jet using the mixing length concept. A semi-empirical equation by *Abramovich [14]* incorporating the effects of density variations using a characteristic velocity is also shown, see also *Chehroudi et al. [9]*.

Brown and Roshko [16] measure spreading for a subsonic two-dimensional incompressible turbulent mixing layer in which helium and nitrogen are used. They make a distinction between mixing layers in which density changes are caused by temperature changes, high-speed compressible (high Mach number and supersonic) flows, and differences in molecular weights (i.e., different gases). In the jet we are investigating here there are both differences in temperature as well as molecular weight except for the N_2-into-N_2 case. Their measurements are shown in Fig. 5. *Papamoschou and Roshko [1]* proposed a theoretical equation for the incompressible variable-density mixing layer as shown in Fig. 5. Finally, *Dimotakis [2]* uses the observation that, in general, the entrainment into the mixing layer from each stream is not the same and, in a system moving with the aforementioned convection velocity, offers a geometrical argument to derive an equation for the two-dimensional incompressible variable-density mixing layer, see Fig. 5.

Because both liquid-like and gas-like visual jet behaviors are observed, the growth rate for liquid sprays produced from single-hole nozzles typical of the ones used in diesel engines are also shown. Because of profound nozzle geometrical effects, *Reitz and Bracco [11]* and *Hiroyasu and Arai [17]*, isothermal-spray angle equations proposed by *Reitz and Bracco [11]* at two different nozzle length-to-diameter ratios, along with their corresponding vertical error-bands indicating experimental scatter around them, are shown in Fig. 5. As a cross check, a recent curve-fitted equation to experimental data from transient sprays proposed by *Naber and Siebers [18]* is also shown. Their angle measurement zone extends beyond our initial region and this to some extent contributes to disagreement seen between the two sets of data for liquid sprays at injector length-to-diameter density ratio of about 4, see Fig. 5.

Figure 5 covers a density ratio of three orders of magnitude, from liquid sprays to supersonic mixing layers, a unique and new plot on its own right. Clearly, within the range plotted, the results of constant spreading angle of incompressible turbulent jet overpredicts nearly all others in Fig. 5. There is also increasing disagreement between turbulent gas jet of *Abramovich [14]* and incompressible variable-density model of *Papamoschou and Roshko [1]* as density ratio increases. To some extent, for measured values, disagreements in this figure can be attributed to differences in the definition of the mixing layer thicknesses and their measurement methods, see *Chehroudi et al. [9]*. It is clear that for a range of density ratios in which our images show gas-jet like appearance, the experimental data agrees well with the proposed theoretical equation by *Papamoschou and Roshko [1]* and closely follows the trend of *Dimotakis [2]*. This can be taken as further and quantitative confirmation that at ambient supercritical pressure and temperature conditions (based on the pure injectant), the injected jets visually behave like a gas though technically it may be referred to as "fluid". To our knowledge, this is the first time such quantitative verification has been demonstrated.

Above the critical condition, there is marked disagreement in both magnitude and slope between liquid sprays (at a comparable length-to-diameter ratio of 85) and our data, see Fig. 5, even though the jet investigated here appears to go through initial phases of the liquid atomization process, see Figs. 3. The reason is that although the jet studied here shows second wind-induced breakup features similar to liquid jets, it fails to reach full atomization state as chamber pressure (really density) is raised. This is because the thermodynamic state approaches the critical point and consequently both surface tension and heat of vaporization are reduced to near-zero values. Transition into the full liquid atomization region is therefore inhibited.

FRACTAL ANALYSIS

In the past ~~ten~~ 10 years, a number of applications of fractal analysis have been demonstrated in different disciplines. For example, *Sreenivasan and Meneveau [19]* compute the fractal dimension of the turbulent/non-turbulent boundary of an incompressible axisymmetric gaseous jet and report a value of 1.33 using two-dimensional slicing by a laser sheet. *Sreenivasan [20]* also reports values of 1.35, 1.34, and 1.38 for a round gaseous jet, a plane gaseous mixing layer, and a boundary layer flow, respectively. Figure 6 shows results of plotting the fractal dimension applied to the N_2-into-N_2 jets as a function of relative chamber pressure. In this figure the fractal dimension by other researchers in the gaseous jets, mixing layer, and boundary layers are also shown for comparison purposes. The interesting part is that the average value measured for our jet reaches very near those of gaseous jets and mixing layers above the critical point of the injectant. This is additional quantitative confirmation of the gaseous jet behavior indicated through our growth rate measurements in this region. As pressure (density) is decreased below P_r of about 0.6, the fractal dimension is rapidly reduced towards the Euclidean value of 1 for a smooth circular cylinder with no surface irregularities. Considering the geometric interpretation of the fractal dimension, measured values are quite consistent with the visual observations of jet interface changes in our tests. For more details see *Chehroudi et al. [21].*

SUMMARY AND CONCLUSIONS

Anatomical changes and growth rates of jets injected into an environment at fixed supercritical temperature but varying pressure from sub- to supercritical are analyzed. As chamber pressure is increased from a low subcritical value, the fluid in the jet appears to go through classical liquid jet breakup stages up to a second wind-induced breakup regime with ligaments and many droplets ejecting from the jet. Penetration into the full atomization regime is inhibited near but before the critical pressure of the injectant because of the combined effects of lowered surface tension and heat of vaporization. At this point the jet assumes a gas-jet like appearance that remains up to the highest pressure tested here. Also, a unique and comprehensive plot on growth rate is formed using most relevant works of others covering an ambient-to-injectant density ratio range of three orders of magnitude. Our measured jet growth rates follow theoretical equations proposed by *Papamoschou and Roshko [1]* and *Dimitakis [2],* both derived for incompressible variable-density gaseous turbulent mixing layers, starting at a pressure near but below the thermodynamic critical pressure of the injectant, *quantitatively supporting the observed gas-jet like visual appearance of the supercritical jets for the first time.* This jet exhibits both liquid-jet like and gas-jet like faces depending on the values of surface tension and heat of vaporization. The appropriateness of the surface tension for liquid jets and sprays and its irrelevance for gaseous jets are among the issues to be reconciled. The first fractal analysis of the jet for the supercritical case also shows agreement with values reported for gaseous jets/mixing layers, another quantitative indication of the gas-jet like behavior.

REFERENCES

[1] **Papamoschou, D. and Roshko, A.** *"The compressible turbulent shear layer: an experimental study,"* J. Fluid Mech., vol. 197, 1988, pp. 453-477.

[2] **Dimotakis, P. E.** *"Two-dimensional shear-layer entrainment,"* AIAA Journal, Vol. 21, No. 11, 1986, pp. 1791-1796.

[3] **Bruno, T. J. and Ely, J. F.** *Supercritical fluid technology*, CRC Press, 1991.

[4] **Newman, J. A. and Brzustowski.** *"Behavior of a liquid jet near the thermodynamic critical region,"* AIAA Journal, vol. 9, 1971, no. 8, pp. 1595-1602.

[5] **Mayer, et al.** *"Injection and mixing processes in high pressure LOX/GH2 rocket combustors,"* AIAA Paper no. 96-2620, ~~Lake Buena Vista, Florida~~, 1996.

[6] **Mayer, et al.** *"Propellant atomization in LOX/GH2 rocket combustors,"* AIAA Paper no. 98-3685, 1998.

[7] **Chen, L.-D. and Sui, P.-C.** *"Atomization during the injection of supercritical fluid into high pressure environment,"* in Mechanics and Combustion of Droplets in Sprays by Chiu and Chigier, Publisher, date

[8] **Woodward, R. D. and Talley, D. G.** *"Raman imaging of transcritical cryogenic propellants,"* AIAA Paper 96-0468, ~~Reno, Nevada~~, January 1996.

[9] **Chehroudi, et al.** *"Initial growth rate and visual characteristics of a round jet into a sub- to supercritical environment of relavance to rocket, gas turbine, and diesel engines,"* AIAA paper 99-0206, ~~Reno, Nevada~~, 1999.

[10] **Schlichting, H.** *Boundary Layer Theory*, MacGraw-Hill Book Company, seventh edition, 1979.

[11] **Reitz, R. D. and Bracco, F. V.** *"On the dependence of spray angle and other spray parameters on nozzle design and operating condition,"* SAE international Congress and Exposition, SAE Paper no. 790494, Detroit, Michigan, February 26-March 2, 1979.
[12] **Faeth, G. M.,** *"Structure and atomization properties of dense turbulent sprays,"* Twenty-third Symposium (International) on Combustion, The Combustion Institute, P.1345, 1990.
[13] **Tseng, et al.** *"Continuous- and dispursed-phase structure of pressure-atomized sprays,"* Progress in Astronautics and Aeronatics: Recent Advances in Spray Combustion, February 1995. publishers
[14] **Abramovich, G. N.** The theory of turbulent jets, M.I.T. Press, 1963.
[15] **Chehroudi, et al.** *"On the Intact Core of Full-Cone Sprays,"* SAE Transaction Paper 850126, 1985.
[16] **Brown, G. and Roshko, A.** *"On density effects and large structure in turbulent mixing layers,"* J. Fluid Mech., vol. 64, 1974, part 4, pp. 775-816.
[17] **Hiroyasu, H. and Arai, M.** *"Fuel spray penetration and spray angle in diesel engines,"* Trans. JSAE, Vol. 21, 1980.
[18] **Naber, J. D. and Siebers, D. L.** *"Effects of gas density and vaporization on penetration and dispersion of diesel sprays,"* SAE Paper no. 960034, 1996.
[19] **Sreenivasan, K. R. and Meneveau, C.** *"The fractal facets of turbulence,"* J. Fluid Mech. Vol. 173, pp. 357-386, 1986.
[20] **Sreenivasan, K. R.** *"Fractals and multifractals in fluid turbulence,"* Annu. Rev. Fluid Mech. Vol. 23, pp. 539-600, 1991.
[21] **Chehroudi, B., Talley, D., and Coy, E.** *"Fractal geometry and growth rate of cryogenic jets near critical point,"* 35th AIAA/ASME/SAE/ASEE joint propulsion Conference, Los Angeles, CA, June 20-24, 1999. (To appear) Use paper number if you have it.

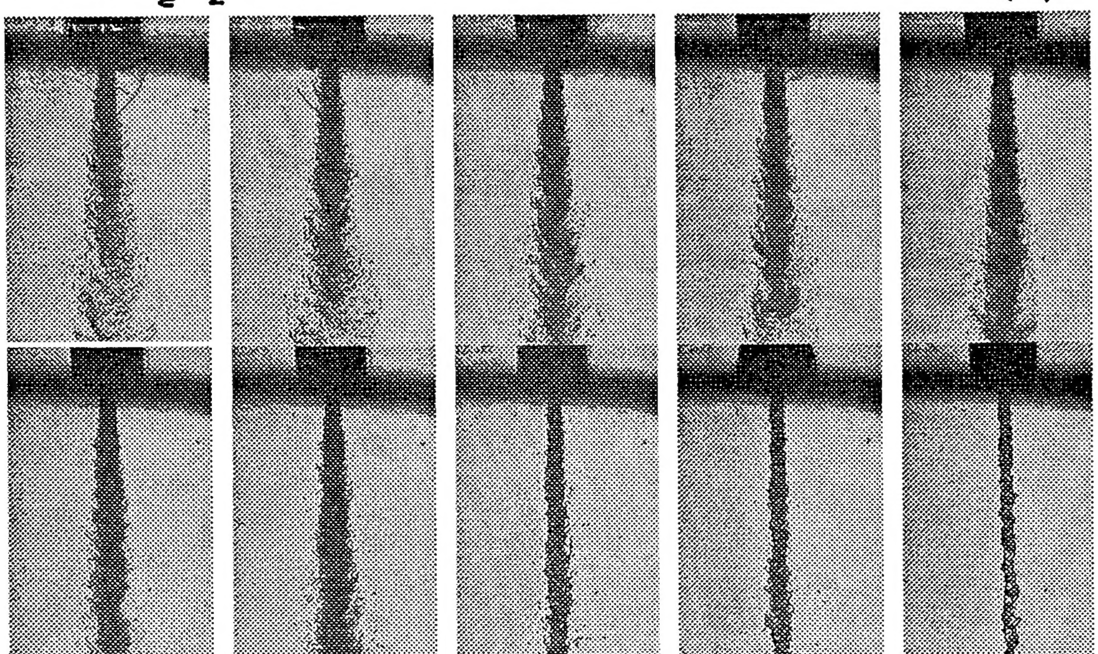

Figure 3. Back-illuminated images of nitrogen injected into nitrogen at a fixed supercritical temperature of 300 K but varying sub- to supercritical pressures ($P_{critical}$ = 3.39 MPa; T_c = 126.2 K). $P_{ch}/P_{critical}$= 2.74, 2.44, 2.03, 1.62, 1.22, 1.03, 0.83, 0.62, 0.43, 0.23; from upper left to lower right. Re= 25,000 to 75,000. Injection velocity: 10-15 m/s. Froud number: 40,000 to 110,000 (momentum-dominated jet). Injectant temperature: 99 to 110 K.

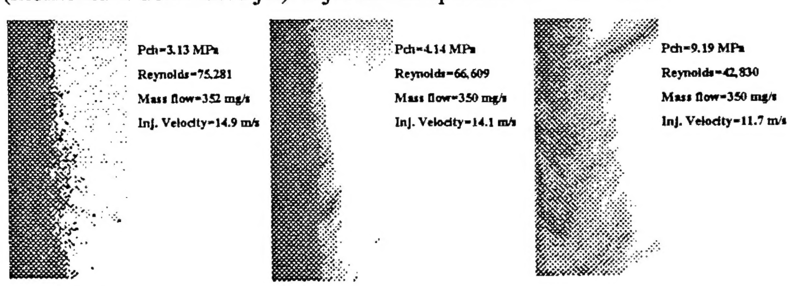

Appearance of conventional breakup of liquid surface indicating ligaments and drops ejecting from the mixing zone

Mixing layer affected by sub- to supercritical transition. No drops are seen

Appearance of Gas/gas mixing layer

Figure 4. Software magnified images of the jet at its outer boundary showing transition to the gas-jet like appearance starting at just below the critical pressure of the injectant. Images are at fixed supercritical chamber temperature of 300 K.

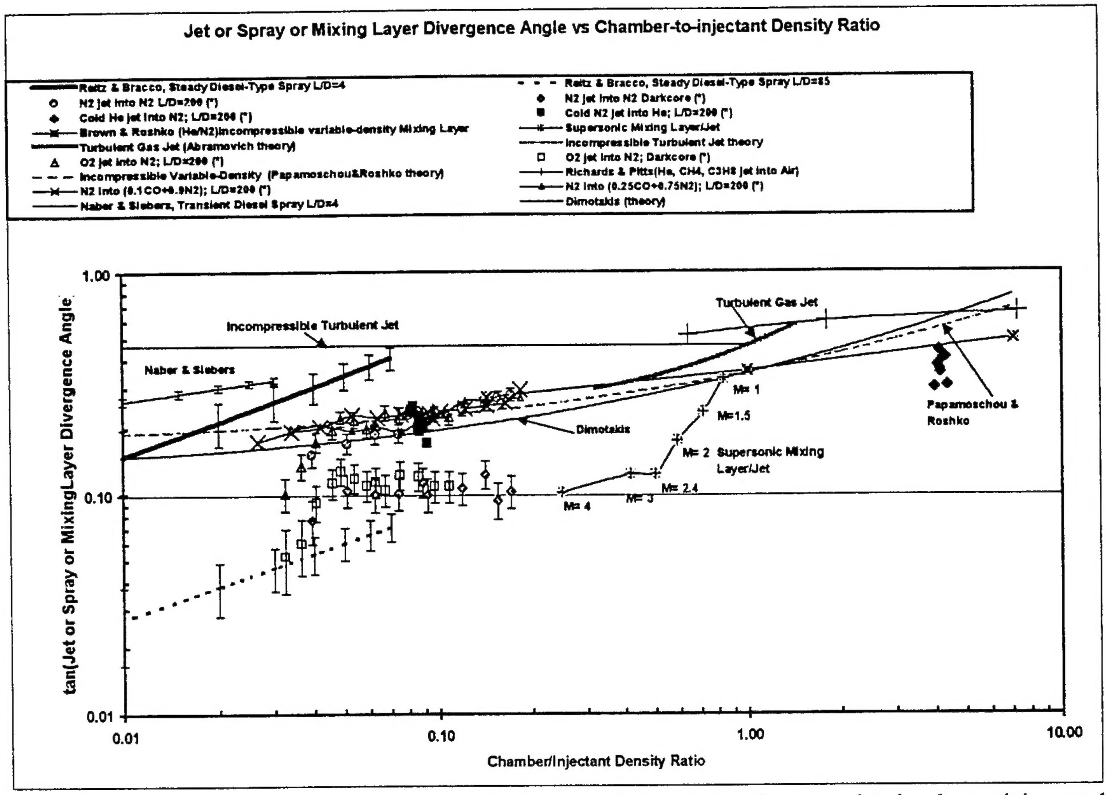

Figure 5. Shows spreading or growth rate as tangent of the visual spreading angle versus the chamber-to-injectant density ratio. (*) refers to data taken at AFRL.

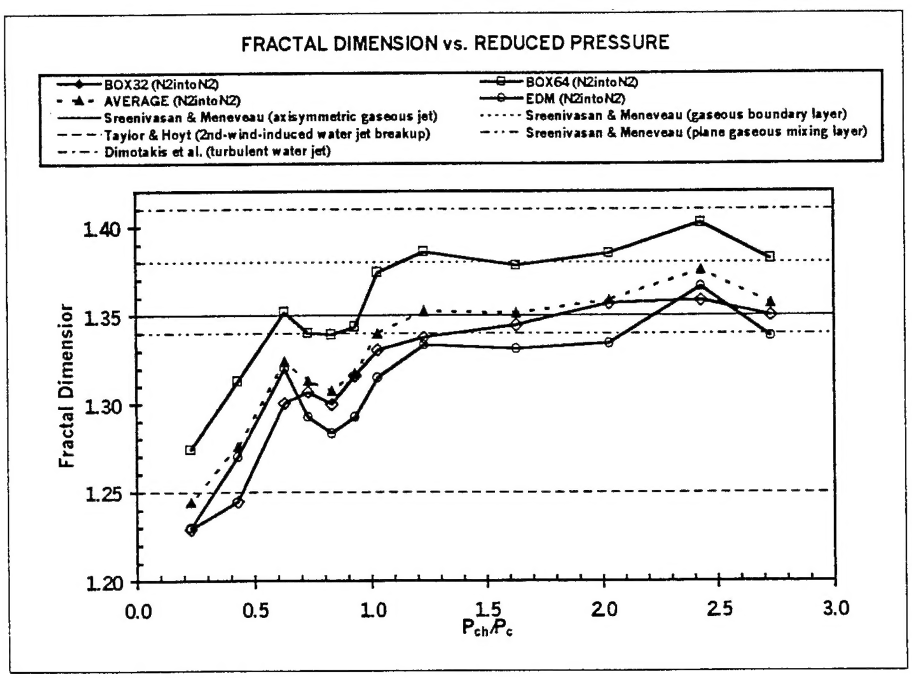

Figure 6. Box-counting and Minkowski (Euclidean Distance Mapping (EDM) algorithm) fractal dimensions of the visual boundary of the jet as a function of the reduced chamber pressure for N_2-into-N_2 injection.